Necklace-State-Mediated Anomalous Enhancement of Transport in Anderson-Localized non-Hermitian Hybrid Systems

M. Balasubrahmaniyam, Sandip Mondal, and Sushil Mujumdar*
Nano-optics and Mesoscopic Optics Laboratory, Tata Institute of Fundamental Research, 1, Homi Bhabha Road, Mumbai 400 005, India

(Received 19 September 2019; revised manuscript received 4 February 2020; accepted 21 February 2020; published 24 March 2020)

Non-Hermiticity is known to manifest interesting modifications in the transport properties of complex systems. We report an intriguing regime of transport of hybrid quasiparticles in a non-Hermitian setting. We calculate the probability of transport, quantified by the Thouless conductance, of hybrid plasmons under varying degrees of disorder. With increasing disorder, we initially observe an expected decrease in average transmission, followed by an anomalous rise at localizing disorder. The behavior originates from the confluence of hybridization and non-Hermiticity, in which the former realizes the aggregation of eigenvalues migrating under disorder, while the latter enables energy transfer between the eigenmodes. We find that the enhanced transmission is mediated by quasiparticle hopping over various Anderson-localized states within the so-formed necklace states. We note that, in this scenario, *all* configurations exhibit the formation of necklace states and enhanced transport, unlike the conventionally known behavior of necklace states which only occurs in rare configurations.

DOI: 10.1103/PhysRevLett.124.123901

Wave transport in mesoscopic systems is a long-standing research area that deals with propagation of waves in a disordered environment [1]. With increasing disorder, the transmission of a wave systematically decreases, leading to various transport regimes such as ballistic, quasiballistic, diffuse, weakly localized, and Anderson localized. Among these, Anderson localization has been one of the central discussions in mesoscopic physics because of its consequence of total arrest of transport, arising from self-interference. Although first proposed in the context of electronic transport [2], Anderson localization has since been observed for a variety of coherent excitations such as matter waves [3], phonons [4], and photons [5–14]. Notably, Anderson localization has always been studied in conservative systems to prevent dissipation that either compromises or masks the consequences of localization. However, real experimental systems are prone to inherent non-Hermiticity arising from scattering, open boundaries, weak absorption, etc. Perhaps the most important consequence of non-Hermiticity is the lifting of orthogonality of eigenmodes, which vitally influences the behavior of complex systems [15–20]. The consequence of non-Hermiticity in disordered systems is now an area of growing interest [21–23], with active interest in non-orthogonality extending to mathematical physics and probability (see Refs. [24–26] and refs therein).

Yet another relatively unexplored facet of localization is the Anderson localization of hybrid quasiparticles [27–32]. Recently, it was shown theoretically that the hybrid setting of a photon-phonon quasiparticle manifests a nontrivial frequency dependence of the localization length, which can provide a convincing evidence of localization even in the presence of dissipation [29]. The experimental challenge of dissimilar propensity of localization of photons and phonons was recently circumvented in GaAs/AlAs random superlattices, carefully designed for maximum spatial overlap of the phonon and photon fields, leading to Anderson colocalization of the phonon-photon quasiparticle [30]. Anderson localization of plasmons at terahertz frequencies [12] was an example of band-edge assisted localization at the hybridization gap [32]. In this work, we reveal an intriguing regime of transport that occurs at the confluence of non-Hermiticity and hybridization. We observe an anomalous enhancement of average transmission in such systems even under localizing conditions. We theoretically and numerically work out the transport in a one-dimensional hybrid plasmonic system under varying disorder. We observe the onset of localization at near-periodic disorder as quantified by the Thouless conductance. The monotonic decrease of conductance with increasing disorder is broken at a certain disorder strength, beyond which the conductance starts rising. This rise occurs despite the individual modes showing a localized character. The analysis of the wave functions reveals that the transport is facilitated by a large population of necklace states in the system. It is known that a necklace state is formed due to the coupling of two or more localized states [33–38] and has a larger spatial extent than determined by the average localization length. In a localizing configuration, the necklace states contribute to the transmission substantially more than the individual localized states [37]. However, the statistical rarity of such modes

does not allow these states to influence the configurationally averaged transport. Our work on hybrid non-Hermitian systems uncovers a hitherto-unknown regime of transport, wherein necklace states are a rule rather than an exception.

The quasiparticle employed in this study is a hybrid plasmon arising from the hybridization of the dispersive surface plasmons [Fig. 1(a), dotted line] with dispersionless cavity resonances (horizontal dashed line). The anticrossing resulting from the hybridization realizes two hyperbolic-dispersive plasmon bands separated by the hybridization gap. The upper band (red line) is radiative and lossy while the lower band (blue line) is nonradiative and supports transport. A characteristic physical system that exhibits such a hybrid dispersion is a linear array of subwavelength cavities in a metallic film, excited at terahertz or microwave frequencies [12,32]. Non-Hermiticity is manifested here due to the metallic loss incurred by the propagating mode. The effective band structure of such a hybridized quasiparticle can be simulated using a modified tight-binding model [27], written as $H_{\mathrm{hp}} = \sum_i [t_{i,i+1} c_i^{\dagger} c_{i+1} + E_i f_i^{\dagger} f_i + V_i c_i^{\dagger} f_i + \mathrm{H.c.}]$, where c is the annihilation operator of the effective Hamiltonian for the plasmon, f is the annihilation operator associated with the cavity resonance, t is the hopping strength, and E is the cavity resonance frequency. V represents the hybridization amplitude of the plasmon with the cavity at each site. This Hamiltonian is matricized into a finite near-diagonal matrix consisting of 100 unit cells.

The cavity resonance frequency E is set to be 0.3 THz, which is the hybridization frequency E_{hy}. The matrix is diagonalized to obtain eigenfrequencies and eigenvectors. The finite size of the system discretizes the continuous hybrid bands into modes. The metallic loss, the source of non-Hermiticity, was invoked after the diagonalization as a broadening of the eigenfrequencies. The variation of the disorder-dependent loss was motivated by our earlier studies [32], approximated with an error function for these calculations [39]. This procedure allows a different loss parameter for every eigenstate, whose magnitude is dependent on the spatial extent of the corresponding eigenvector. The total loss length is typically one or two orders larger than the system size, and hence does not inhibit transport. Figure 1(b) shows the calculated density of states (DOS) around E_{hy}. The broad asymmetric peak at the band edge below 0.3 THz is the remnant of the van Hove singularity (marked by the lower dashed red line), originating from the aggregation of lower order modes of the finite system at the band edge. This feature in the density of states is essentially responsible for surface-bound transport at low frequencies in metals where plasmon polaritons cannot be excited. The isolated peaks away from E_{hy} originate from the isolated higher order modes of the finite system. The inset emphasizes the hybridization gap ΔE, which, in this case was about 0.02 THz. The upper dashed red line marks the peak in the DOS due to the upper band, which is highly radiative.

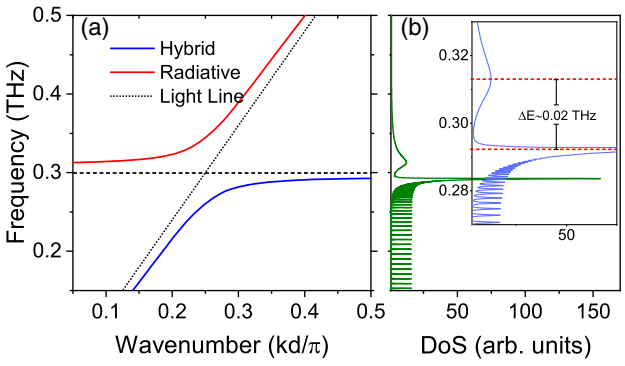

FIG. 1. (a) Dispersion of hybrid plasmon polariton bands, with the propagating lower band (blue line) and radiative upper band (red line) resulting from the anticrossing of plasmon dispersion (dotted line) and the cavity mode (dashed line). (b) Calculated density of states for a finite system, with the hybridization gap emphasized in the inset.

For the periodic system, $V_i = V_0$, the unperturbed splitting, set here to 0.05 THz. Disorder is invoked by randomizing the V_i, representing random spacing between the cavities. For a strength of disorder δ, the value of each V_i is incremented by a uniformly distributed random number from $[-\delta \cdot V_0/2, \delta \cdot V_0/2]$. Under disorder, the modes in the transmission bands migrate into the hybridization gap. The migration of four modes (averaged over 10 000 configurations) closest to the band edge as a function of δ is shown in Fig. 2(a). As can be seen, the migration of each mode is limited to E_{hy}. Therefore, the eigenfrequencies all congregate at strong disorder. The configurationally averaged DOS also reflects the saturation in the form of an emergent peak, as seen in Fig 2(b). The green curve indicates the behavior of the near-periodic system. The van Hove singularity and the neighboring peaks for the bound modes are seen, along with a broad pedestal at high frequency (~0.32 THz), which corresponds to the radiative mode. As disorder increases, the DOS shows a tail in the hybridization gap (blue curve). Figure 2(c) depicts the DOS for a single configuration. Significantly, at $\delta = 0.95$, even for a single configuration, a band of frequencies is observed close to E_{hy}. This band is realized by the spectral overlap of migrating modes even within one configuration. While the width associated with an individual mode is ~0.2 GHz, the width of the emergent band ~1.2 GHz, a factor of ~6 times larger. Although such minibands have been theoretically discussed for necklace states in strong disorder [33], they only allude to occasional, rare configurations. Our system exhibits the miniband in every configuration under strong disorder. The broadband nature of the DOS peak implies a higher group velocity compared to the localized modes, which leads to faster transport through the system even at strong disorder [33]. The non-Hermiticity realizes a spectral overlap between the eigenmodes, lifting their orthogonality.

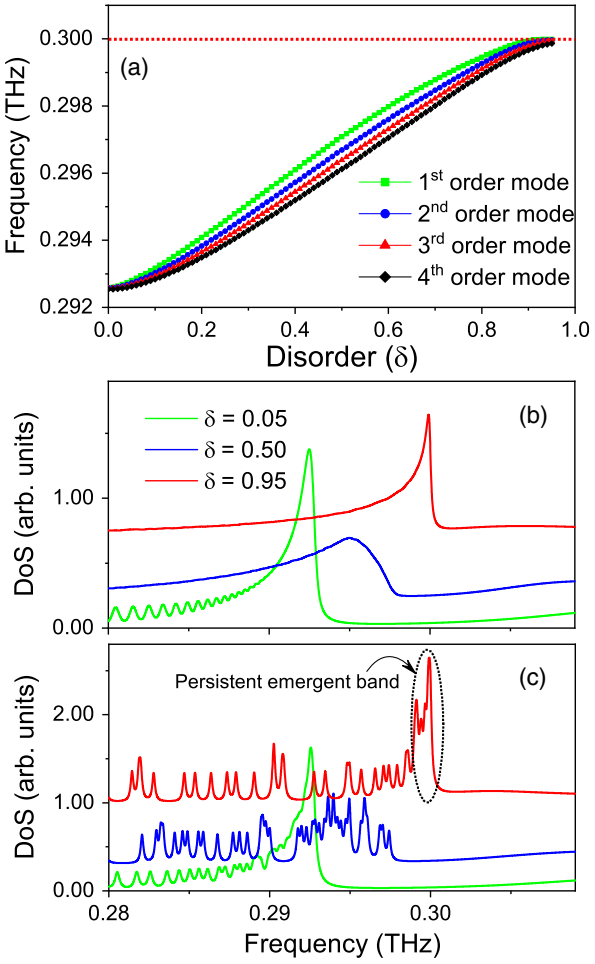

FIG. 2. (a) Migration of a few nonradiative band edge modes with increasing disorder. (b) Configurationally averaged DOS close to E_{hy} for three disorder strengths. (c) DOS for an individual configuration for the same disorder strengths, emphasizing the emergent band at strong disorder.

In one-dimensional systems with minimal loss, the Thouless number can be employed as a direct measure of conductance [41]. The Thouless number is calculated as $g = \delta\omega/\Delta\omega$ where $\delta\omega$ is the average spectral width of two neighboring modes, and $\Delta\omega$ is their spectral separation. Here, the g is calculated for eight modes that eventually form the emergent band at the band edge for different configurations. The variation of $\langle g\rangle$ with disorder is presented in Fig. 3 (red circles). For comparison, $\langle g\rangle$ calculated for modes of a (nonhybrid) dielectric system is also shown (black squares). Under weak disorder, $\langle g\rangle > 1$ for both systems. The $\langle g\rangle$ reduces with increasing disorder, and close to $\delta \sim 0.23$, $\langle g\rangle$ becomes less than 1, indicating incipient localization. This corresponds to the near-periodic disorder. Beyond $\delta = 0.5$, the behavior of $\langle g\rangle$ of the hybridized system deviates from that of the dielectric system. While the latter goes deeper into localization, the $\langle g\rangle$ of the hybrid plasmonic system exhibits an unusual increment with disorder. The nonmonotonic variation

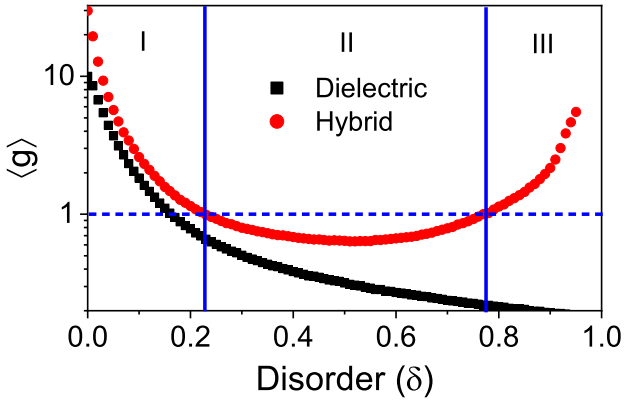

FIG. 3. Thouless conductance $\langle g\rangle$ with disorder strength in the vicinity of E_{hy} for the hybrid plasmonic (red circles) and the dielectric (black squares) system. Dashed blue line indicates $\langle g\rangle = 1$, demarcating localization regime for the hybrid system (vertical blue lines).

crosses 1 again at $\delta \sim 0.77$. This reveals an unexpected enhancement of transport in the presence of strong disorder, where Anderson localization should actually occur. Eventually, at 95% disorder, the $\langle g\rangle \gg 1$, representing a situation of strongly delocalized modes despite localizing disorder.

The physical origin of this phenomenon can be traced to the effect of disorder on the hybrid particle. For conventional particles like photons in a coupled-resonator (-waveguide) system, the energy exists only in photonic form. So, any introduced disorder in coupling between resonators (or waveguides) also results in change in the on-site energies. This allows the energy of the disordered modes to occupy any position on the energy axis. In comparison, for our hybrid system, the on-site energy is photonic, while coupling is plasmonic. Hence, the disorder in coupling terms does not affect the on-site photonic resonant energy. As a result, the energy of the disorder modes are limited to the resonant energy of the cavities. This induces the coalescence of eigenvalues under disorder, resulting into a miniband and enhancement of transport.

To investigate the mode structure creating the anomalous transport, we analyzed the eigenfunctions of the structures. Commensurate with the physics of localization, we observed eigenmodes with exponential decays wherein the decay got tighter with increasing disorder [39]. However, for the current hybrid-plasmonic system, the transport in the miniband is determined by the contribution of multiple eigenmodes that have a finite amplitude at that frequency. Accordingly, the intensity profile at a particular frequency ω is calculated as $|\phi(z,\omega)|^2 = |\sum_i \mathcal{L}_i(\omega)\psi_i(z)|^2$, where $\mathcal{L}_i(\omega)$ is the amplitude at ω of the Lorentzian corresponding to the ith eigenvalue with an associated eigenvector $\psi_i(z)$. Figure 4 shows the calculated intensity distribution at the edge-most peak of the DOS [shown in Fig 2(c)] for three disorder strengths. For near-periodic disorder, the intensity

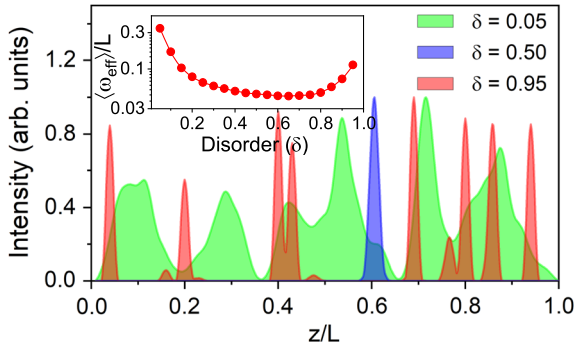

FIG. 4. Intensity profile at the band edge at three disorders. Inset: Effective width of the intensity distribution (log Y axis) at the band edge as a function of disorder.

distribution shows a spatial profile extended over the length of the system (green plot). For intermediate disorder, a single tightly localized mode appears roughly in the central region of the structure (blue plot), commensurate with the $\langle g \rangle < 1$ in Fig 3. For strong disorder, a multipeaked distribution is seen (red plot), where each peak essentially shows a tightly localized character. However, the overall wave function is extended over the entire structure. This is a manifestation of a necklace state, where each exponentially localized mode is likened to a bead of a necklace [35]. While this represents the intensity in one configuration, the inset depicts the configurationally averaged behavior, represented as disorder dependence of effective mode width $w_{\text{eff}} = \{[(\sum_{i=1}^{N} I_i)^2]/[\sum_{i=1}^{N} I_i^2]\}$, where i is the site number. With increasing disorder, the w_{eff} initially drops and reaches a minimum value at intermediate disorder, representing the tightest localization. Subsequently, it increases again at stronger disorder, depicting delocalized behavior. This is in agreement with that of $\langle g \rangle$ shown in Fig 3, and reveals the origin of the enhancement in transport in the wave functions. We note that these wave functions are reminiscent of the multifractal states characterized by formation of minibands at strong disorder in systems with long-range hopping [42–44].

With the computation of $|\phi|^2$, the origins of the enhanced transport are clear. A single exponentially localized eigenfunction implies maximum occupation probability of the quasiparticle at the peak, with exponentially decaying probability away from the peak. For the hybrid quasiparticle, the wave function essentially comprises multiple localized modes in the neighbourhood, due to which the quasiparticle is able to hop between the neighboring localized eigenstates. To explicitly verify this situation in a realistic system, we simulated a one-dimensional coupled resonator waveguide for hybrid plasmons. Figure 5 elucidates the situation therein. The schematic of the structure is shown in plot 5(a), which depicts the array of subwavelength cavities in a metallic thin film [39]. This system has been experimentally shown to sustain Anderson localization at terahertz frequencies [12,32]. The black curve in Fig. 5(b) depicts the intensity distribution when radiation at

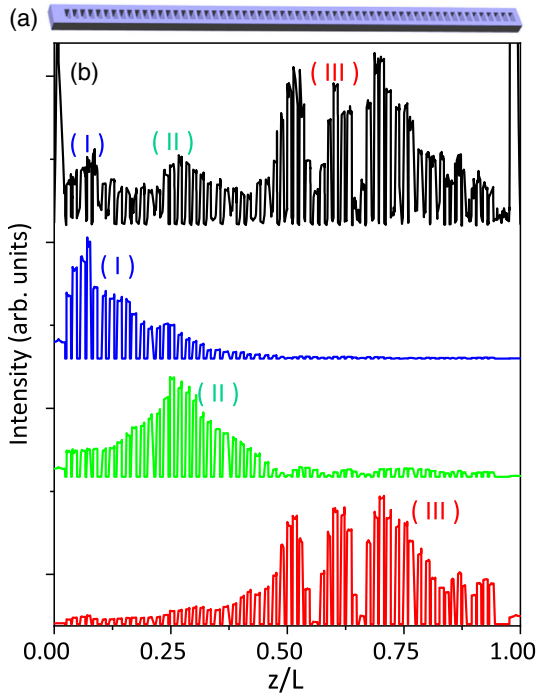

FIG. 5. (a) Schematic of a hybrid-plasmonic coupled resonator waveguide. (b) Intensity distribution (black curve) at a frequency ω at strong disorder in a configuration comprises three ψ_i's labeled I (blue), II (green), and III (red). The transmission occurs through hopping via localized states.

frequency ω is incident from the input (left) end of the array under strong disorder. Multiple peaks are seen in the intensity distribution. Eigensolver analysis of the structure provides three eigenfunctions (labeled as I, II, and III) at the frequency ω sustained in this configuration, shown in the lower (blue, green, and red) curves. Each eigenmode is very weakly coupled to either end of the structure, which implies minimal transmissivity of the individual mode. However, the non-Hermitian nature of the hybrid system ensures a spectrospatial overlap between them, which allows the quasiparticles to hop through the localized states and undergo transmission. The intensity profile in black is seen to be a necklace of the three eigenmodes.

The hopping probability between neighboring eigenmodes is determined by the proximity of the modes. We, hence, quantify the average behavior of the mode proximity under strong disorder in the tight-binding algorithm. The separation s between the various peaks in the necklace states is measured, and the distribution of peak spacings $[P(s/\bar{s})]$ computed over 10 000 configurations is plotted in Fig. 6. The distribution is seen to peak at $s/\bar{s} = 0.27$, and decays exponentially. Importantly, $P(s/\bar{s}) \neq 0$ as $s/\bar{s} \to 0$, revealing that eigenmodes can be in arbitrarily close proximity. This situation leads to an anomalous enhancement in transport. We studied the behavior of the necklace states for increasing sample size, and found that the number of localized states (or "beads" in the "necklace") increase

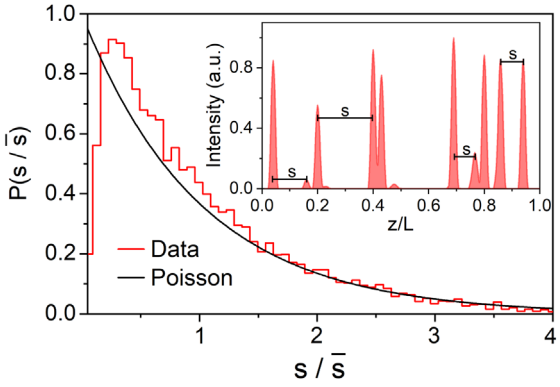

FIG. 6. Distribution of the mean separation between the peaks at $\delta = 0.95$ (red curve). Black curve: Poisson distribution. Inset: Representative $|\phi|^2$, illustrating the separations.

linearly with sample size. Hence, it may be extrapolated that such anomalous transport mediated through necklace states can exist in arbitrarily large samples [39], permitted by the loss.

In summary, we have uncovered an interesting realm of transport in non-Hermitian hybrid systems. We have analyzed strongly disordered hybrid plasmonic systems, wherein an anomalous enhancement of transmission is observed at the hybridization frequency. The transmission is facilitated via a statistical abundance of necklace states, comprising multiple exponentially localized eigenstates. The quasiparticle is transported through hopping over the various localized states. Consequently, the average transport is enhanced, characterized by a Thouless conductance much larger than 1. We believe this work marks a significant development in the physics of non-Hermitian mesoscopic systems.

We acknowledge discussions with Kedar Damle, Vikram Tripathi, and Rajdeep Sensarma. We acknowledge funding from the Department of Atomic Energy, Government of India (12-R&D-TFR-5.02-0200). S. Mujumdar acknowledges the Swarnajayanti Fellowship from the Department of Science and Technology, Government of India.

M. B. and S. Mondal contributed equally to this work.

*mujumdar@tifr.res.in; http://www.tifr.res.in/~mujumdar.

[1] P. Sheng, *Introduction to Wave Scattering, Localization, and Mesoscopic Phenomena* (Academic Press, San Diego, 1995).
[2] P. W. Anderson, Phys. Rev. **109**, 1492 (1958).
[3] J. Billy, V. Josse, Z. Zuo, A. Bernard, B. Hambrecht, P. Lugan, D. Clément, L. Sanchez-Palencia, P. Bouyer, and A. Aspect, Nature (London) **453**, 891 (2008).
[4] H. Hu, A. Strybulevych, J. H. Page, S. E. Skipetrov, and B. A. van Tiggelen, Nat. Phys. **4**, 945 (2008).
[5] D. S. Wiersma, P. Bartolini, A. Langedijk, and R. Righini, Nature (London) **390**, 671 (1997).
[6] M. Segev, Y. Silberberg, and D. N. Christodoulides, Nat. Photonics **7**, 197 (2013).
[7] C. Conti and A. Fratalocchi, Nat. Phys. **4**, 794 (2008).
[8] L. Sapienza, H. Thyrrestrup, S. Stobbe, P. D. Garcia, S. Smolka, and P. Lodahl, Science **327**, 1352 (2010).
[9] Y. Lahini, A. Avidan, F. Pozzi, M. Sorel, R. Morandotti, D. N. Christodoulides, and Y. Silberberg, Phys. Rev. Lett. **100**, 013906 (2008).
[10] T. Sperling, W. Buehrer, C. Aegerter, and G. Maret, Nat. Photonics **7**, 48 (2013).
[11] T. Schwartz, G. Bartal, S. Fishman, and M. Segev, Nature (London) **446**, 52 (2007).
[12] S. Pandey, B. Gupta, S. Mujumdar, and A. Nahata, Light Sci. Appl. **6**, e16232 (2017).
[13] R. Kumar, M. Balasubrahmaniyam, K. Shadak Alee, and S. Mujumdar, Phys. Rev. A **96**, 063816 (2017).
[14] S. Mondal, R. Kumar, M. Kamp, and S. Mujumdar, Phys. Rev. B **100**, 060201(R) (2019).
[15] J. T. Chalker and B. Mehlig, Phys. Rev. Lett. **81**, 3367 (1998).
[16] H. Cao and J. Wiersig, Rev. Mod. Phys. **87**, 61 (2015).
[17] O. Xeridat, C. Poli, O. Legrand, F. Mortessagne, and P. Sebbah, Phys. Rev. E **80**, 035201(R) (2009).
[18] Y. V. Fyodorov and D. V. Savin, Phys. Rev. Lett. **108**, 184101 (2012).
[19] Y. V. Fyodorov and B. Mehlig, Phys. Rev. E **66**, 045202(R) (2002).
[20] H. Schomerus, K. M. Frahm, M. Patra, and C. W. J. Beenakker, Physica (Amsterdam) **278A**, 469 (2000).
[21] J. Wang and A. Z. Genack, Nature (London) **471**, 345 (2011).
[22] M. Davy and A. Z. Genack, Nat. Commun. **9**, 4714 (2018).
[23] M. Davy and A. Z. Genack, Phys. Rev. Research **1**, 033026 (2019).
[24] Y. V. Fyodorov, Commun. Math. Phys. **363**, 579 (2018).
[25] P. Bourgade and G. Dubach, arXiv:1801.01219.
[26] Z. Burda, J. Grela, M. A Nowak, W. Tarnowski, and P. Warchol, Phys. Rev. Lett. **113**, 104102 (2014).
[27] H.-Y. Xie, V. E. Kravtsov, and M. Müller, Phys. Rev. B **86**, 014205 (2012).
[28] H.-Y. Xie and M. Müller, Phys. Rev. B **87**, 094202 (2013).
[29] T. F. Roque, V. Peano, O. M. Yevtushenko, and F. Marquardt, New J. Phys. **19**, 013006 (2017).
[30] G. Arregui, N. D. Lanzillotti-Kimura, C. M. Sotomayor-Torres, and P. D. García, Phys. Rev. Lett. **122**, 043903 (2019).
[31] J. H. García, B. Uchoa, L. Covaci, and T. G. Rappoport, Phys. Rev. B **90**, 085425 (2014).
[32] M. Balasubrahmaniyam, A. Nahata, and S. Mujumdar, Phys. Rev. B **98**, 024202 (2018).
[33] J. Bertolotti, S. Gottardo, D. S. Wiersma, M. Ghulinyan, and L. Pavesi, Phys. Rev. Lett. **94**, 113903 (2005).
[34] P. Sebbah, B. Hu, J. M. Klosner, and A. Z. Genack, Phys. Rev. Lett. **96**, 183902 (2006).
[35] J. B. Pendry, Adv. Phys. **43**, 461 (1994).
[36] L. Chen, W. Li, and X. Jiang, New J. Phys. **13**, 053046 (2011).
[37] J. Bertolotti, M. Galli, R. Sapienza, M. Ghulinyan, S. Gottardo, L. C. Andreani, L. Pavesi, and D. S. Wiersma, Phys. Rev. E **74**, 035602(R) (2006).
[38] M. Ghulinyan, Phys. Rev. A **76**, 013822 (2007).

[39] See Supplemental Material at http://link.aps.org/supplemental/10.1103/PhysRevLett.124.123901: Sec. S1 for disorder dependence of the loss; Sec. S2 for disorder dependence of the degree of localization; Sec. S3 for finite-element method based analysis of the structure, which includes Ref. [40]; Sec. S4 for system-size dependence of the necklace states.
[40] S. Pandey, S. Liu, B. Gupta, and A. Nahata, Photonics Res. **1**, 148 (2013).
[41] D. J. Thouless, Phys. Rev. Lett. **39**, 1167 (1977).
[42] V. E. Kravtsov, I. M. Khaymovich, E. Cuevas, and M. Amini, New J. Phys. **17**, 122002 (2015).
[43] P. A. Nosov, I. M. Khaymovich, and V. E. Kravtsov, Phys. Rev. B **99**, 104203 (2019).
[44] M. Pino, V. E. Kravtsov, B. L. Altshuler, and L. B. Ioffe, Phys. Rev. B **96**, 214205 (2017).